

LA-UR-12-20388

Approved for public release; distribution is unlimited.

Title: Stopped Pion Absorption by Medium and Heavy Nuclei in the Cascade-Exciton Model

Author(s): Mashnik, Stepan G

Intended for: MCNP6 references package



Disclaimer:

Los Alamos National Laboratory, an affirmative action/equal opportunity employer, is operated by the Los Alamos National Security, LLC for the National Nuclear Security Administration of the U.S. Department of Energy under contract DE-AC52-06NA25396. By approving this article, the publisher recognizes that the U.S. Government retains nonexclusive, royalty-free license to publish or reproduce the published form of this contribution, or to allow others to do so, for U.S. Government purposes. Los Alamos National Laboratory requests that the publisher identify this article as work performed under the auspices of the U.S. Department of Energy. Los Alamos National Laboratory strongly supports academic freedom and a researcher's right to publish; as an institution, however, the Laboratory does not endorse the viewpoint of a publication or guarantee its technical correctness.

Stopped Pion Absorption by Medium and Heavy Nuclei in the Cascade-Exciton Model

Stepan G. Mashnik^{1,*}

¹*International Centre for Theoretical Physics, Trieste, Italy*

Abstract

A large variety of experimental data on stopped negative pion absorption by nuclei from C to Bi (energy spectra and multiplicities of n, p, d, t, ³He and ⁴He; angular correlations of two secondary particles; spectra of the energy release in the “live” ²⁸Si target on recording protons, deuterons and tritons in the energy range 40-70 MeV, 30-60 MeV and 30-50 MeV, respectively; isotope yields; momentum and angular momentum distributions of residual nuclei) are analyzed within the framework of the cascade-exciton model of nuclear reactions. Comparison is made with other up-to-date models of the process. The contributions of different pion absorption mechanisms and the relative role of different particle production mechanisms in these reactions are discussed.

We reproduce here this 1992 ICTP Report as it represents a historical interest as a realization of the Cascade-Exciton Model (CEM) to describe stopped pion absorption, and was and still is used in dozens of countries all over the world. E.g., the current CEM03.03 and LAQGSM03.03 event-generators of the latest LANL Monte Carlo transport code MCNP6 have today modified parts from the FORTRAN code of that old version of CEM.

*Current and permanent address: XCP-3, Computational Physics Division, Los Alamos National Laboratory, Los Alamos, NM 87545, USA

REF ID: A6



INTERNATIONAL CENTRE FOR THEORETICAL PHYSICS

STOPPED PION ABSORPTION BY MEDIUM AND HEAVY NUCLEI IN THE CASCADE-EXCITON MODEL

S.G. Mashnik



INTERNATIONAL
ATOMIC ENERGY
AGENCY



UNITED NATIONS
EDUCATIONAL,
SCIENTIFIC
AND CULTURAL
ORGANIZATION

MIRAMARE-TRIESTE



International Atomic Energy Agency
and
United Nations Educational Scientific and Cultural Organization
INTERNATIONAL CENTRE FOR THEORETICAL PHYSICS

STOPPED PION ABSORPTION BY MEDIUM AND HEAVY NUCLEI
IN THE CASCADE-EXCITON MODEL *

S.G. Mashnik **

International Centre for Theoretical Physics, Trieste, Italy.

ABSTRACT

A large variety of experimental data on stopped negative pion absorption by nuclei from C to Bi (energy spectra and multiplicities of n , p , d , t , 3He and 4He ; angular correlations of two secondary particles; spectra of the energy release in the "live" ^{28}Si target on recording protons, deuterons and tritons in the energy range 40-70 MeV, 30-60 MeV and 30-50 MeV, respectively; isotope yields; momentum and angular momentum distributions of residual nuclei) are analyzed within the framework of the cascade-exciton model of nuclear reactions. Comparison is made with other up-to-date models of the process. The contributions of different pion absorption mechanisms and the relative role of different particle production mechanisms in these reactions are discussed.

MIRAMARE – TRIESTE

March 1992

* Partially presented at the Workshop on Computation and Analysis of Nuclear Data Relevant to Nuclear Energy and Safety, ICTP, Trieste, Italy, 10 February–13 March 1992.

** Adress after 20 March 1992: Laboratory of Theoretical Physics, Joint Institute for Nuclear Research, Head Post Office P.O. Box 79, 101000 Moscow, Russia.

Permanent address after 23 December 1994: Academy of Sciences of Moldavia, Institute of Applied Physics, Grosul Str. 5, 277028, Kishinev, Moldavia.

1. Introduction

Stopped negative pion absorption in atomic nuclei occupies an important place in intermediate energy physics as it touches different aspects of nuclear structure, especially those concerning the role of correlations between the nucleons in the nuclei and the high-momentum components of nuclear wave functions. These reactions have been under investigation for about four decades, but an unambiguous interpretation of the observed phenomena has not yet been found [1, 2].

The law of energy and momentum conservation forbids the absorption of a pion by a free nucleon. In principle, a stopped negative pion can be absorbed by an intranuclear proton, but for this process a momentum of ~ 500 MeV/c is required for the proton [1]. Because this value is far beyond the Fermi momentum of about 250 MeV/c, the reaction will be strongly suppressed. Single nucleon absorption may manifest itself (see, for example, review [2]) in the energy spectrum of nucleons, since in this case a nucleon must possess maximum energy as compared to nucleons formed in other absorption mechanisms. In the case of light nuclei, single nucleon absorption gives rise to a peak in the high-energy "tail" of the spectrum. The probability of single nucleon absorption measured in this way [3] for 6Li , 7Li and ^{12}C is $\sim 2 \cdot 10^{-3}$. In the region of heavy nuclei, due to high density of excited states of residual nuclei, it is impossible to identify the peak corresponding to single nucleon absorption. The probability for single nucleon absorption may be estimated only indirectly as a deviation of experimental data from the calculations based on the two nucleon absorption mechanism. Rough estimation [4] gives for the value of single nucleon absorption probability $\leq 10^{-3}$.

More accurate estimates for the probability of single nucleon absorption in heavy nuclei may be obtained by the activation methods. The yields of reactions (π^- , n) and (π^- , p) measured in [5, 6] also prove to be small and equal to $\sim 10^{-3} - 10^{-4}$.

The knowledge of the probability of pion absorption on a single nucleon is very important for finding out the presence of pion condensate in nuclei [7]. According to [8] the rescattering of intranuclear nucleons by spin-isospin density fluctuations is likely to cause the pion single nucleon absorption to be ~ 100 - 1000 times enhanced. Apparently the small probability $\leq 10^{-3}$ for this process found in [3]-[6] indicates on the absence of pion condensate in finite normal nuclei.

The most of the existing experimental (see, for example [9]-[22]) and theoretical (see, for example [2, 4], [18]-[32]) data lead to the conclusion that the two-nucleon absorption mechanism predominates in intermediate and heavy nuclei. But even in this case there are serious discrepancies between estimates of an important parameter relating to the dynamics of the process, namely, the ratio R of the probabilities of absorption by np and pp pairs, both for a particular nucleus [14, 23] and as a function of atomic number [26].

At the same time, the role of absorption by heavy internal nuclear clusters has remained unclear. For example, the inclusive spectra of composite particles for some nuclei are reproduced equally satisfactorily by models which describe the pickup process on the nuclear surface by two-nucleon absorption mechanism [28]-[30], by pre-equilibrium models [4], [18]-[21], [24, 26, 31, 32], in a pure phenomenological way by coalescence model [33] and also by models in which the composite particles are the primary products of quasi-free absorption by intranuclear clusters with a number of nucleons more than two [34, 35]. In order to discriminate, to some extent between existing theoretical models (see review of modern models, for example, in [26]), it seems necessary to compare theory with experiment for an appreciable number of characteristics. Note, in this connection, the results of the published [36] study for 6Li , which has shown that neither the two-nucleon mechanism with subsequent pickup nor cluster models can explain most of the correlation data on composite-particle yields and the recent careful analysis [21] of the composite-particle yields for Be , C , Si , Cu and Ge targets, which has shown that the present theoretical

suggestions on the mechanisms of their formation cannot explain the entire set of experimental data.

Two opposed methods are usually used to estimate the probabilities of pion absorption by heavy clusters from the comparison of experimental data with model calculations:

A) In the first scheme one supposes the *a priori* existence of some multinucleon absorption mechanisms with the corresponding probabilities (see, for example [37, 38]). One calculates characteristics of the process for different values of these probabilities and, after that, one defines the best ones from the best agreement with experimental data.

B) In the second method one calculates sensible to the absorption mechanisms characteristics by taking into account only the two nucleon pion absorption. After that, one estimates the probabilities for other absorption mechanisms indirectly, from the deviations of the corresponding experimental characteristics from the calculated ones (see, for example [18, 21, 24]).

Though in the first scheme one may obtain a better description of the experimental data, the introduction of several additional free parameters in the models (see, for example [38]) make the results obtained by this method insufficiently reliable.

Therefore in this work we will follow the second method. We will consider in the cascade-exciton model (CEM) of nuclear reactions [39] only the "background" two-nucleon absorption mechanism in a large range of nuclear target masses. We will calculate and compare with experiment and other models various characteristics and will discuss the relative role of different interaction mechanisms for these processes.

2. The Main Concepts of the Model

We calculate here stopped negative pion absorption by intermediate and heavy nuclei by taking into account only the two-nucleon absorption mechanism. The characteristics of an intranuclear nucleon pair absorbing a pion are determined from the Fermi distribution in which the dependence of the Fermi level on the position of the point of absorption is taken into account. The nucleon density in the nuclear interior is determined from the two-parameter Fermi distribution

$$n(r) = q [1 + \exp(r - \bar{r})/b]^{-1}, \quad (1)$$

where q is a normalizing constant and \bar{r} , b are parameters whose value for our nuclei can be found in [40]. It is assumed that the radial distribution $n(r)$ is the same for neutrons and protons:

$$n_n(r)/n_p(r) = N/Z. \quad (2)$$

The point at which the pion is absorbed in the nucleus was determined from the distribution derived in [27] from calculations on pionic atoms

$$P_{abs} \sim \exp[-(r - c)^2/2\sigma^2]. \quad (3)$$

The values of constants c and σ were determined by interpolating between the results given in [27] for nearby nuclei.

After the absorption, the pion mass m_π has the form of kinetic energy of primary nucleons, each having the energy $E = m_\pi/2$ in the center of mass system. In the c.m.s. primary nucleons fly apart isotropically in the opposite directions. In the laboratory system, the energy of primaries will have certain deviation about the quantity $m_\pi/2$ due to momentum of intranuclear nucleons.

Depending on their directions and the point at which pion is absorbed, nucleons may escape from the nucleus either without interaction ("primary emission") or undergoing one or several collisions with intranuclear nucleons. This stage is similar to ordinary nuclear reaction when an intermediate energy nucleon incident on a nucleus initiates an intranuclear cascade.

To describe these processes we will use the cascade-exciton model (CEM) of nuclear reaction [39], which satisfactorily predicts [41] the energy spectra, angular distributions and double differential cross sections of nucleons and composite particles emitted in nucleon-nucleus interactions at intermediate energies. A detailed description of the CEM may be found in [39]. Therefore, only its basic assumptions are considered below. The CEM assumes that the reactions occur in three stages. The first stage is the intranuclear cascade in which primary particles can be rescattered a number of times prior to absorption by, or escape from the nucleus. The excited residual nucleus formed after the emission of the cascade particles determines the particle-hole configuration that is the starting point for the second, pre-equilibrium stage of the reaction. The subsequent relaxation of the nuclear excitation is treated in terms of the exciton model of pre-equilibrium decay, which includes the description of the equilibrium evaporative stage of the reaction.

An important point of CEM is the condition for passing from the intranuclear cascade stage to pre-equilibrium emission. In the conventional cascade-evaporation models the fast particles are traced up to some minimal energy, the cut-off energy T_{cut} , being about 7-10 MeV, below which particles are considered to be absorbed by the nucleus. In the CEM it is suggested to use another criterion according to which a primary particle is considered as a cascade one, namely the proximity of an imaginary part of the optical potential $W_{opt.mod.}(r)$ calculated in the cascade model to be appropriate experimental value $W_{opt.exp.}(r)$. This value is characterized by the parameter

$$\mathcal{P} = |W_{opt.mod.} - W_{opt.exp.}|/W_{opt.exp.} \quad (4)$$

In this work the value $\mathcal{P} = 0.3$ is used extracted from the analysis [41] of experimental nucleon-nucleus data at intermediate energies.

One should note that in the CEM the initial configuration for the pre-equilibrium decay (number of excited particles and holes, i.e., excitons $n_0 = p_0 + h_0$, excitation energy E^* and linear momentum \mathbf{P} of the nucleus) differs strongly from that usually postulated in the exciton models (see review [26]) values: $n_0 = 4$, $p_0 = 2$, $h_0 = 2$; $\mathbf{P} = \mathbf{P}_0 = \mathbf{0}$; $E^* = [m_\pi + M(Z, N) - M(Z - 1, N + 1)]/c^2$. Our calculations [32, 41] show that the distributions of residual nuclei formed following pion absorption after the cascade stage of the reaction, i.e., before the pre-equilibrium emission with respect to n_0 , p_0 , h_0 , E^* and \mathbf{P} are rather broad.

The version of CEM [39] used here assumes that composite particles are formed only as a result of coalescence of excited nucleons at the pre-equilibrium stage of the reaction and of evaporation from compound nuclei.

In case of nucleon-nucleus interactions the CEM predicts asymmetrical angular distributions for secondary particles. Firstly, this is due to high asymmetry of cascade component. A possibility to have asymmetrical distributions for nucleons and composite particles emitted during the pre-equilibrium interaction stage is related to keeping some memory of the direction of a projectile. It means that along with the energy conservation law we need to take into account the conservation law of linear momentum \mathbf{P} at each step when a nuclear state is getting complicated. In a phenomenological approach this can be realized in different ways [39]. The simplest way used here consists in sharing a bringing-in after cascade stage momentum \mathbf{P} (similarly to excitation energy E^*) between an ever increasing number of excitons involved into interaction in the course of equilibration of the nuclear system. In other words, the momentum \mathbf{P} should be attributed only to n excitons rather than to all A nucleons. Then, particle emission will be isotropic in the

proper n -exciton system, but some anisotropy will arise in both the laboratory and center-of-mass reference frame.

This feature of the CEM allows use of the model for description of angular correlations for two particles emitted after pion absorption by nuclei. Such a possibility is inaccessible for the majority of up-to-date models.

Our calculations were performed with fixed values of the level-density parameter a_0 of the excited nucleus. These values were close to the experimental values for the pion-absorbing nuclei. The numerical values of \bar{r} , b , c , σ and a_0 are given in [19, 26]. The other CEM parameter values are fixed and the same as in [39].

Note that in the CEM, in contrast to some other models (see, for example [24, 33]) which include a free parameter for normalization, the calculations are performed with an absolute normalization. The Monte Carlo CEM method simulates the absorption of the pion by a nucleus, so that it can be used to describe simultaneously an extensive set of reaction characteristics.

The particle yield in our model is given by

$$Y_{CEM} = (Y_{CEM}^{pp} + R Y_{CEM}^{np}) / (R + 1), \quad (5)$$

where Y_{CEM}^{pp} and Y_{CEM}^{np} are the particle yields accompanying absorption of pp and np pairs, respectively.

It is useful to extract from R the statistical factor taking into account the number of np and pp pairs in a nucleus containing N neutrons and Z protons. When the radial density of neutrons and protons in the nucleus is the same, i.e., (2) is valid, we have

$$R = [2N/(Z - 1)]R' \equiv R_0 R', \quad (6)$$

where R' is the ratio of the absorption widths for the np and pp pairs:

$$R' = \Gamma(\pi^- np \rightarrow nn) / \Gamma(\pi^- pp \rightarrow np). \quad (7)$$

Since the dynamics of absorption by nucleon pairs in a particular spin-isospin state is not well understood, a purely theoretical determination of R' is hardly possible at present. The up-to-date experimental data also can not clarify this question (see, for example review [26]). The interpretation of the value of the R is therefore dual in character. Thus, R can be regarded as a free parameter of the theory that can be used with (5) to normalize the theoretical particle yields to the experimental data. The fact that this normalization is possible is not at all trivial because the physical value of R must be positive, and this occurs only when the experimental yield lies between the theoretical yields calculated for absorption by pp ($R = 0$) and by np ($R = \infty$) pairs. The value of R obtained in this way and, consequently, the value of R' can probably be looked upon as a physical result characterizing the absorption process.

3. Results and Discussions

3.1. Energy Spectra of Nucleons

Nucleons emission following pion absorption is an important type of decay of highly excited nuclei. We have analyzed [4], [18]-[22], [26, 31, 32, 41] in the CEM most of the recent measurements of energy spectra of neutrons [15, 16, 42, 43, 44] and protons [11]-[16], [21, 47] emitted after absorption of stopped pions by intermediate and heavy mass nuclei. As an example, in fig. 1 are shown the energy spectra of nucleons formed after π^- -absorption in ^{40}Ca and ^{59}Co .

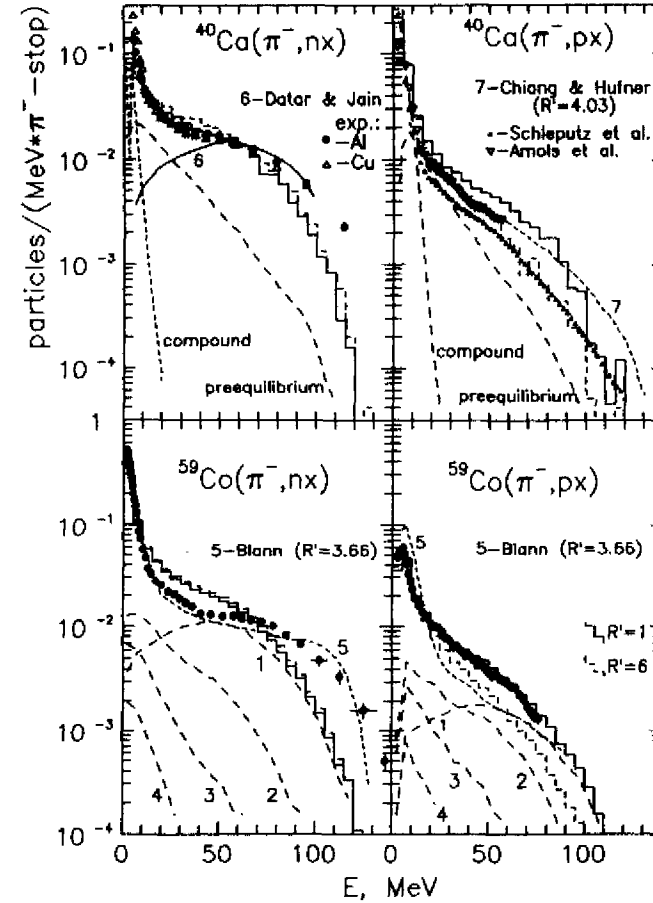


Fig.1. Energy spectra of nucleons emitted after the absorption of stopped π^- by ^{40}Ca and ^{59}Co . Experimental data: n : ^{40}Ca - [42], ^{59}Co - [43]; p : ^{40}Ca - [11, 45], ^{59}Co - [14]. Calculations: The contribution of all three (cascade, pre-equilibrium and evaporative) CEM components are drawn by the solid ($R'=1$) and dashed ($R'=6$) histograms. For ^{40}Ca the evaporative and the pre-equilibrium components are shown by dashed lines. For ^{59}Co dashed curves 1, 2, 3 and 4 show the contributions from cascade ($R'=1$) nucleons of 1st, 2nd, 3rd and ≥ 4 th generation, i.e., from primary nucleons and nucleons emitted after one, two, and three or more collisions with intranuclear nucleons, respectively. The lines 5, 6 and 7 show calculations from [25], [30] and [29], respectively.

The experimental spectra have a specific feature attributed to existence of fast cascade, in-

intermediate pre-equilibrium and slow evaporative stages of π^- -absorption. Three components, "evaporative", intermediate and fast nucleons are distinct in the spectra. The evaporative part includes nucleons emitted by excited residual compound nuclei, the high-energy one includes fast cascade particles emitted from the surface layer of the nucleus mainly without collisions with intranuclear nucleons ("primary" nucleons) and the intermediate energy spectrum is composed of nucleons emitted at the cascade and pre-equilibrium stages of the reaction. For heavy targets the evaporative component of the proton spectra is poorly distinct due to the effect of the Coulomb barrier.

The surface character of absorption results in weak dependence in shape and absolute magnitude of high-energy portion of the nucleons spectra on the atomic number of the nucleus-target. Thus, the experimental mean multiplicities of "direct" neutrons for ^{12}C , ^{59}Co and ^{197}Au are 1.45 ± 0.10 , 1.38 ± 0.11 and 1.32 ± 0.10 neutrons per absorbed pion [43]. The yields of fast protons ($E_p > 70$ MeV) measured in [22] for C, Si and Cu also very weakly depend on the nucleus-target and are 0.015 ± 0.003 , 0.020 ± 0.003 and 0.018 ± 0.003 , respectively.

The CEM fairly predicts the increasing of the evaporative and the pre-equilibrium neutron emissions with increasing of the nucleus-target mass and, on the whole, satisfactorily describes both the shape and the absolute magnitude of neutron spectra. However, the fast neutron yields are systematically underestimated by our model for every nucleus-target considered. This presumably points to insufficiently correct description of high momentum component of nucleon distribution in nucleus [35]. The local density approximation used in the CEM gives small momentum of nucleons of the nucleus at its periphery and, hence, insignificant "smearing" of the neutron spectra.

This may be proved by the microscopic calculations of Datar and Jain [30] for energy spectra of primary neutrons (for ^{40}Ca , see fig.1) or by simplified calculations of fast component in the neutron spectra made by Mukhopadhyay *et al.* [46] on the assumption that one of the neutrons formed after pion absorption by a pair of nucleons goes out of nucleus without interactions, while the other is absorbed by it. Momentum distribution of intranuclear nucleons in the form $f(p) \sim \exp(-p^2/\alpha^2)$ used in [46], where the value $13 \text{ MeV} \leq \alpha^2/2M_n \leq 20 \text{ MeV}$ (M_n is nucleon mass) allows better description of the high-energy part of the neutron spectra. The remain discrepancy for $110 \text{ MeV} \leq E_n \leq 140 \text{ MeV}$ may presumably be explained by the small contribution ($\sim 10^{-3} - 10^{-4}$) of other mechanisms of pion absorption, single-nucleonic mechanism among them.

For comparison, together with the experimental data and the CEM predictions for $R' = 1$ and $R' = 6$, in figure 1 are also shown the pre-equilibrium [25], the cascade [23] and the microscopic [30] calculations. One can see that quite different models reproduce equally satisfactorily the inclusive spectra of nucleons. This means that the inclusive spectra are not really sensitive enough to initial assumptions, and, to determine the role of different reaction mechanisms, we must consider not only inclusive measurements on individual nuclei, but also other particle-emission characteristics.

As $R \gg 0$, much more primary neutrons are usually emitted during the cascade stage of the reaction than primary proton ones. As a result of this, the calculated energy spectra of neutrons are insensitive to the value of R' , when the high energy part of the proton spectra appreciable depends on R' (see fig.1). Note in this aspect the analysis [26] of the experimental proton spectra measured for various targets by different groups [11]-[16], [47], which has shown that either R' is sensitive enough to nuclear structure of the targets, or there are significant contradictions between the absolute normalization of proton spectra measured by different workers. To clarify this question in [26] it was proposed to measure in the frame of the same method and with good energy resolution and statistics energy spectra of protons emitted after stopped π^- absorption by different nuclei (including different isotopes of the same elements). Such measurements for Be,

C, Si, Cu and Ge have been performed recently by Gornov *et al.* [22].

Fig.2 shows these experimental proton spectra together with our CEM calculation and the results reported by other authors.

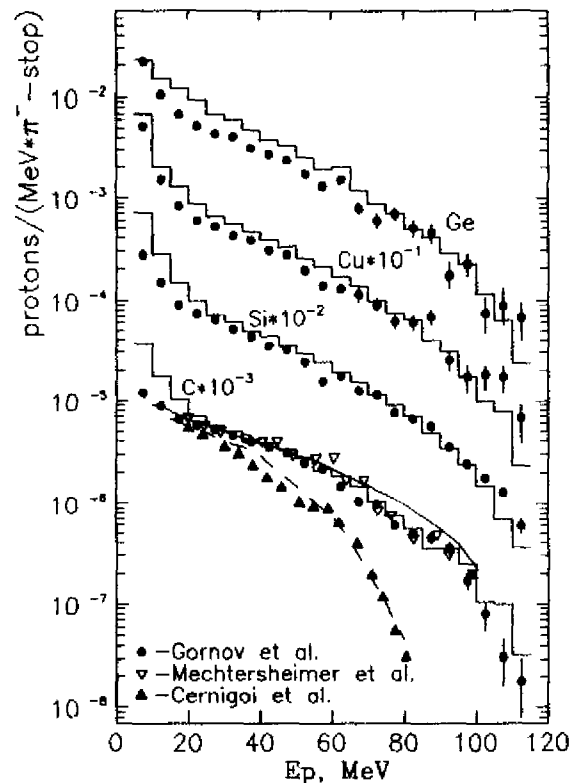


Fig.2. Inclusive energy spectra of protons: \bullet -[22], ∇ -[12], \blacktriangle -[16], histograms - CEM calculations ($R' = 3.5$), solid curve - calculation from [23], dashed curve - calculation based on the α -particle model [35].

All CEM spectra shown in fig.2 were obtained for $R' = 3.5$. It is clear that the theoretical and experimental spectra are in satisfactory agreement in a wide energy range and for these experimental data we do not observe some evident dependence of R' on the mass of nucleus-target. For ^{12}C our calculation is in agreement with calculation from [23] and experimental data [12, 22], but not with calculation based on the α -particle model [35] and Cernigoi *et al.* data [16]. This means that the conclusion about the α -particle mechanism of proton production on ^{12}C , reported in the latter paper, is confirmed neither by recent measurement [22], nor by our calculation.

The spectra of protons from ^{28}Si are analyzed in greater detail in fig.3.

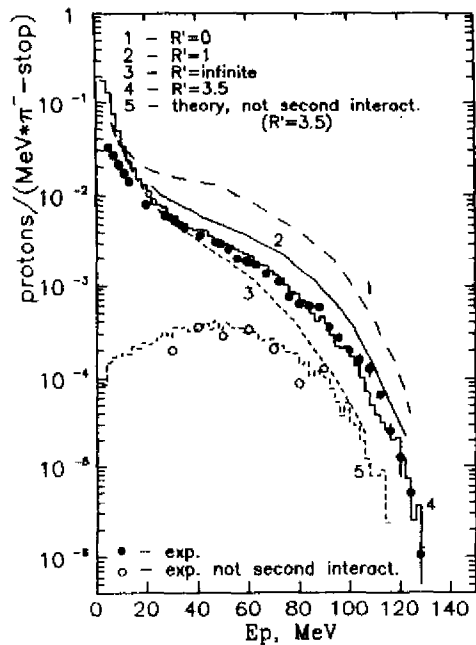


Fig.3. Energy spectra of protons emitted as a result of absorption of negative pions by ^{28}Si nuclei: ●- experimental inclusive spectrum [22], ○- experimental spectrum for events without interactions in the nuclear interior [22]. Solid histogram - CEM calculation ($R'=3.5$), dashed histogram - CEM calculation for events without secondary interactions in the interior of the nucleus ($R'=3.5$). The curves 1, 2 and 3 show the CEM calculations with $R'=0, 1$ and ∞ , respectively.

The value of R' obtained from (5) decreases smoothly from 5.0 to 2.0 as the lower limit of the energies is varied from 40 to 100 MeV. This range of variation of R' appear to be a measure of uncertainty in the result obtained by this method. The mean value is $R' = 3.5 \pm 1.5$. We note that use of the method whereby R' is determined from the ratio of proton yields for different part of spectra [23] does not improve the accuracy. It can be seen from fig.3 that the curve corresponding to $R' = 1$ is clearly not in agreement with the proton experimental data. At the same time the $R' = 1$ neutron spectra are reproduced quite well [2, 26]. This situation is due to the low sensitivity of the neutron spectra to the value of R' . Thus, at $E = 50$ MeV, the calculated in the CEM proton spectra for $R' = 0$ and ∞ differ by almost an order of magnitude (see, fig.3), whereas the neutron spectra differ only a factor of 1.5.

3.2. Energy Spectra of Composite Particles

On great interest is the investigation of spectra of composite particles, as it is a common practice to consider that such particles may be formed due to pion absorption in a more complicated,

in contrast to two-nucleon, association. But before studying this problem for complex nuclei, we must elucidate the contribution of other possible mechanisms to the formation of those particles.

Evaporation is the simplest among those mechanisms. In this case a composite particle is emitted by a highly-excited compound nucleus at the last stage of the process. The calculations [31] have shown that none of the composite particles spectra can be obtained in this case either in shape or in absolute value.

At the same time, our CEM calculations [4], [18]-[22], [26, 31, 32, 41] have shown that pre-equilibrium processes make an important contribution to the spectra of composite particles. As an example, in fig.4 are shown measured by Gornov *et al.* [21] energy spectra of $d, t, {}^3\text{He}$ and ${}^4\text{He}$ emitted after stopped pion absorption by $\text{C}, \text{Si}, \text{Cu}$ and Ge together with our CEM calculations and the results of other authors [14, 28, 29].

As we can see in fig.4 the CEM satisfactorily reproduces the spectra of composite particles for ^{28}Si , with the exception of the underestimated yield of α -particles (which is inherent in most models for any nuclei), and also of deuterons with energies higher than 30 MeV. The agreement for Cu and Ge is somewhat worse. The disagreement, in particular for Cu , increases with energy of particles. Note that in the simplified (in comparison with the CEM) Machner exciton model [24] also one observes a decrease, relative to the experimental data, of the yield of composite particles with energy, particularly if we take into account the method of normalization of [24]. For ^{12}C (fig.4) the agreement also does not seem to be satisfactory enough, which apparently is associated with limitations in the applicability of the CEM to light nuclei.

As seen from fig.4 the contribution of pre-equilibrium particles to spectra is large, but at high energies our calculated spectra lie, as a rule, below the experimental ones. It is possible that the discrepancy in this region may eliminate both the above mechanism of direct emission following pion capture on multinucleonic associations, and the mechanism of composite particle emission at the stage of intranuclear cascade. The latter processes may involve intranuclear nucleon pickup with a fast nucleon as well as knocking-out of beforehand prepared clusters in nucleus by fast nucleons.

It should be noted that the considered mechanisms of composite particle emission (pre-equilibrium emission, pickup and knockout process) must also show themselves in the case of inelastic proton-nucleus interaction with $E_0 \sim m_\pi/2$. Therefore, to estimate the fraction of composite particles emitted following pion absorption by the multinucleon association (for example, by the α -cluster), it would be advisable to use the results of proton-nuclear experiments in this analysis. Thus, the experiments performed at proton energy $E_0 = 62$ MeV [49], 72 MeV [50] and 90 MeV [51] have shown that spectra of $d, t, {}^3\text{He}$ and ${}^4\text{He}$ in proton-nuclear and pion-nuclear interactions have similar shape. This points to a great contribution of secondary processes to composite particle emission.

3.3. Yields of Secondary Particles

Though the yields of particles emitted following pion absorption by nuclei are integral characteristics, their careful investigation permits to find out certain information about the reaction mechanisms.

For example, in fig.5 are represented the R' -dependence of proton yields calculated in the CEM for C, Si , and Cu targets with the aid of (5). The points denote the values of R' for which the calculated yields coincide with the experimental ones [19]. One can see that the values of R' obtained in this way for different nuclei are close to one another, and agree with the found above value $R' = 3.5 \pm 1.5$, independently of the lower energy limit.

We have also determined [22] R' from the yield ratio for high-energy protons and neutrons.

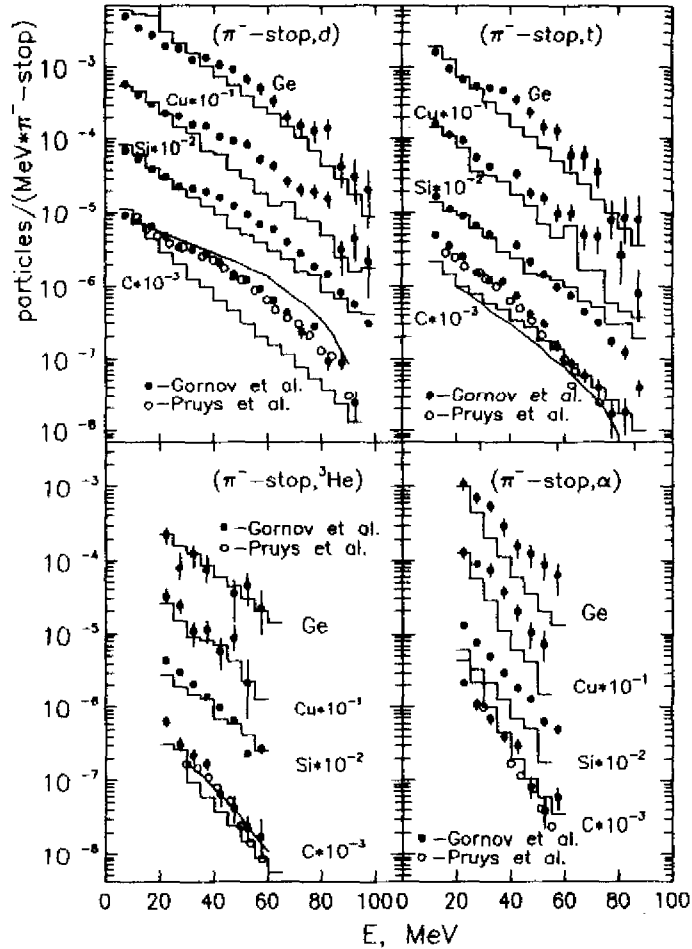


Fig.4. Inclusive energy spectra of deuterons, tritons, ^3He and ^4He . Experimental data: \bullet -[21], \circ -[14]; the histograms are CEM calculation ($R'=3.5$), and the solid curves are the calculation according to the pickup model [28, 29].

Assuming that these are primary particles, we have

$$R = 1/2(Y_n/Y_p - 1). \quad (8)$$

The neutron data were taken from [42], which gives a detailed analysis of the experimental situation and indicates possible reasons for discrepancies between results reported by different

workers. The final data are listed in table 1. It is clear from the table that the tendency for R' calculated from (8) to increase with increasing limiting energy, which was noted in [14], is also shown by Gornov *et al.* data [22]. The value $R' \leq 1$ obtained in [14] for low limiting energies ($E = 20$ MeV) is obviously too low because secondary particles provide a large contribution to the proton spectra as compared with the neutron spectra (see fig.1). The value of R' at high energies ($E = 70$ MeV), at which secondary processes are less appreciable, are found to be closer to the values for light nuclei.

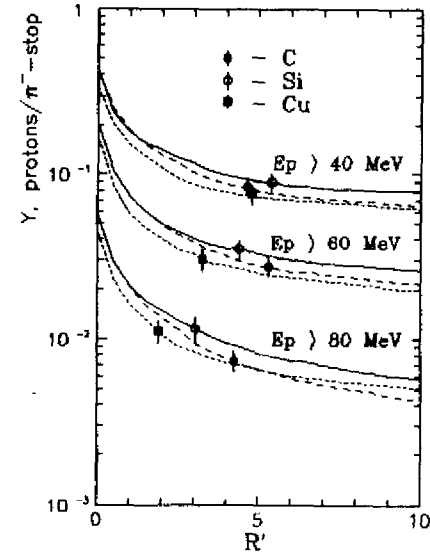


Fig.5. The R' -dependence of proton yield. Point - experimental data [19], curves- CEM calculation.

The measured proton yield increases with increasing A up to a maximum near ^{40}Ca , and thereafter declines slowly [9, 10]. We have analyzed [22] the A -dependence of the proton yield from the standpoint of the two-nucleon absorption mechanism, using a variable related to the probability of absorption on a pp pair. This variable was taken to be $\beta = (Z-1)/(Z-1+2R'N)$, i.e., the probability of pion capture by a pp pair for the same value of R' for all nuclei. Figure 6 shows a plot of this function for protons with $E_p \geq 50$ MeV. In addition to Gornov *et al.* data [22], we also reproduce the relative measurement reported in [10]. The latter are normalized to Gornov *et al.* data [22], using the total yield of the Be , C , and Si nuclei. It is clear that the proton yields increase monotonically with increasing β , and, between carbon and copper, the yields lie (to within experimental error) on a straight line passing through the origin and the point representing the yield of ^{28}Si . We note that the function $Y_p(\beta)$ remains linear in a rather wide range of energy

(30-70 MeV). We also find that, if

$$Y_p(E_p > 50 \text{ MeV}) = \frac{1}{2}(Z-1)/(Z-1+2R'N), \quad (9)$$

then the value of R' deduced from (9) is close to the values obtained by the methods discussed above ($R' = 3.5$ for ^{28}Si).

Table 1

Yields of neutrons [42] and protons [22] [%/ π^- -stop] and the ratio of probabilities of absorption on np and pp pairs.

| A | Y_n | Y_p | R | R_0 | R' |
|------------|---------|-----------|-----------|-------|-----------|
| E > 40 MeV | | | | | |
| C | 91 ± 11 | 8.1 ± 1.0 | 5.1 ± 1.3 | 2.4 | 2.1 ± 0.6 |
| Si | 75 ± 9 | 8.8 ± 1.1 | 3.8 ± 1.0 | 2.154 | 1.8 ± 0.5 |
| Cu | 73 ± 9 | 7.3 ± 0.9 | 4.5 ± 1.1 | 2.788 | 1.6 ± 0.4 |
| E > 70 MeV | | | | | |
| C | 27 ± 6 | 1.5 ± 0.3 | 8.9 ± 3.8 | 2.4 | 3.7 ± 1.6 |
| Si | 30 ± 6 | 2.0 ± 0.3 | 7.1 ± 2.8 | 2.154 | 3.3 ± 1.3 |
| Cu | 33 ± 6 | 1.8 ± 0.3 | 8.9 ± 3.1 | 2.786 | 3.2 ± 1.2 |

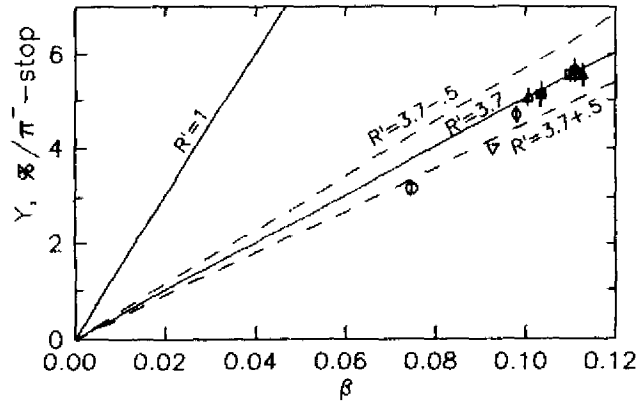


Fig. 6. Yield of protons with energies above 50 MeV. Experimental data: \circ - Be, ∇ - Ge, \diamond - Cu, \triangle - C and \square - Si - from [21]; \blacksquare - Al, \bullet - S and \blacktriangle - Ca - from [10]. Lines - CEM calculation.

It is thus clear that the above systematization of experimental data on proton yields shows that R' is constant for the nuclei that were examined here and provides a natural explanation

of the above A -dependence of the yield of high-energy protons in terms of the pair mechanism. Analysis of the results published by other workers shows that most of them are consistent with the hypothesis that R' is constant. For example, it follows from the linear dependence (9) that the proton-yield maximum should be observed for ^{40}Ca (the heaviest stable isotope for which $N = Z$), which is in agreement with [9, 10].

We note that the values of R' for intermediate nuclei are close to the figure of 4.0 ± 0.5 obtained by exclusive measurements on ^3He [52], i.e., the lightest nucleus for which absorption on np and pp pairs is possible. On the other hand, further measurement on other targets, especially different isotopes of the same elements, would be useful as a means of elucidating the range of validity of the above properties. For example, further data on ^9Be and Ge that depart from the linear dependence would be interesting. In our view, there are different reasons for this. In ^9Be , which has a cluster structure, there are significant pion-absorption mechanisms that do not lead to the production of fast protons [19]. In Ge , in which the number of neutrons is much greater than the number of protons ($N - Z = 10$), there may be a departure from the statistical ratio of number of np and pp pairs in the surface layers of the nucleus [53].

From point of view of the two-nucleon absorption mechanism in the CEM the yields of composite particles are less informative. For example, in table 2 are shown the yields of charged particles in the absorption of π^- mesons by ^{28}Si [18]. One can see that the CEM predicts an appreciable fraction of the measured composite particle yields, but the results of calculation are practically insensible to the value of R' . The reason for this is the assumption of used here version of CEM [39], in accordance with which composite particle are produced only as a result of coalescence of excited nucleon at pre-equilibrium stage of reaction and of evaporation.

Table 2

Experimental [18] and theoretical yields of charged particles emitted after π^- -absorption in ^{28}Si [%/ π^- -stop].

| | Y_p | Y_d | Y_t | Y_{He} | Y_α |
|---------------|-------------|------------|------------|-----------|------------|
| E=(20-70) MeV | | | | | |
| Experiment | 18.0 ± 1.8 | 7.44 ± .74 | 1.76 ± .18 | .65 ± .08 | 1.57 ± .17 |
| CEM (R=7.5) | 22.0 ± .2 | 5.50 ± .10 | 1.60 ± .10 | .47 ± .06 | .73 ± .07 |
| CEM (R=0) | 60.6 ± .6 | 5.90 ± .10 | 1.40 ± .10 | .60 ± .06 | .81 ± .07 |
| CEM (R=∞) | 16.9 ± .2 | 5.40 ± .10 | 1.60 ± .10 | .45 ± .06 | .72 ± .07 |
| E=(40-70) MeV | | | | | |
| Experiment | 6.38 ± .69 | 2.64 ± .26 | .47 ± .05 | .12 ± .02 | .21 ± .03 |
| CEM (R=7.5) | 8.23 ± .10 | 1.40 ± .10 | .40 ± .06 | .11 ± .02 | .08 ± .02 |
| CEM (R=0) | 30.10 ± .50 | 1.80 ± .10 | .38 ± .08 | .15 ± .02 | .12 ± .02 |
| CEM (R=∞) | 5.31 ± .08 | 1.40 ± .10 | .41 ± .06 | .10 ± .02 | .08 ± .02 |

But to discriminate the mechanisms of composite particles formation the A dependence of their yields are greatly informative. So, our comparison [21] of the experimental results on the emission of composite particles with calculations shows that the theoretical models of the mechanisms of their formation elaborated up to day cannot explain the entire set of Gornov *et al.* data [18] - [21]. The different behavior of A dependence of the yields of composite particles, probably, manifests various mechanisms of their formation. The ratio of the t and ^3He yields, which for the first time was measured in a broad range of nuclei [19, 21], is inconsistent with the model

of production of these particles as the result of pickup reactions. The substantial increase of the yields of t in ^{12}C , and particularly in ^9Be , indicates the increasing role of absorption by α clusters. However, the influence of clustering in light nuclei on the process of absorption of stopped π^- mesons cannot be reduced to the quasi-free absorption by an intranuclear α particle, and new mechanisms are required to be involved to explain the A dependence of the yields and spectra of composite particles.

3.4. Correlation Between Emitted Particles

Important information on the mechanism of pion absorption in nuclei has been obtained from the measurement of energy and angular distributions of various particles in coincidence (see [43, 47, 48] and their references). Angular correlations of two neutrons or of a neutron and proton have a sharp maximum at an angle of 180° for light ^6Li , ^7Li and ^{12}C nuclei which becomes wider for heavier nuclei ^{59}Co and ^{197}Au [43, 48]. The picture such as that corresponds to a two-nucleon mechanism of pion absorption and is fairly described in the approach using the model of intranuclear cascades [4, 23, 27] and CEM [26, 41]. The energy spectrum of one neutron in coincidence with another one [43, 48] or with one proton [48] has a wide maximum for ^6Li , ^7Li and ^{12}C nuclei at 50-60 MeV, which also indicates a two-nucleon absorption mechanism.

On the other hand, the opening angle distributions of $(n-d)$ and $(n-t)$ [48], or $(p-d)$ and $(p-t)$ [47] pairs detected in coincidence also have a very sharp maximum near 180° for ^6Li and ^7Li and a wider one, for ^{12}C , ^{59}Co and ^{197}Au . This may be looked as an indication of pion absorption on α -clusters or other multinucleon associations in nuclei.

However, it should be remarked that in coincidence measurements of two fast particles emitted in reaction $\pi^-_{\text{stop}} + A$ only from the law of momentum conservation one should expect a preferential outgoing back to back, even if particles are independently emitted at different stages of reaction (as $\mathbf{P}_0 = 0$). It is of interesting to estimate the contribution of this purely kinematic "background" effect to the measured angular correlations of different secondary particles. As we regard here only the pion absorption by two nucleons and CEM permits to describe the angular distribution both of nucleons and composite particles, we can use with this aim in view the CEM.

As an example, in figure 7 a part of measured in [47, 48] angular distributions of two coincident fast particles ($E_{n,p,d,t} > 20\text{MeV}$, $E_{\alpha,\text{He},\alpha} > 35\text{MeV}$) emitted after π^- -absorption in ^{59}Co is compared with our CEM calculation. In table 3 are presented the experimental and calculated yields for emission of two coincident fast particles in the same reaction.

It is clear from fig.7, and table 3, CEM gives a correct description of $(n-n)$, $(n-p)$ and $(p-p)$ angular correlations and yields. Note that calculated here opening angle distributions for primary $(n-n)$ and $(n-p)$ particles are sharper than for all nucleons, but the contribution of primary nucleons to measured $(n-n)$ and $(n-p)$ angular correlations in the CEM is much smaller than in the simplified (in comparison with the CEM) Chiang and Hüfner model [23].

If calculated yields of one fast neutron in coincidence with another fast particle are practically insensitive to the value of R' , the yields of one fast proton in coincidence with the second fast particle (especially, if the last is also an proton) are very dependent on the value of R' . The CEM calculations agree better with experimental correlation data [47, 48] for $R' \simeq 2$, which is close to the figure $R' = 3.5 \pm 1.5$ obtained above from the analysis of energy spectra of protons.

One can see from fig.7 and table 3, the "background" uncorrelated consecutive emission of two fast particles predicted by CEM contributes essentially to the measured in coincidence characteristics also in the case when the second detected particle is composite, and what is more, even when both detected particles are composite. In these cases predicted by CEM angular distributions are

some broader than experimental ones.

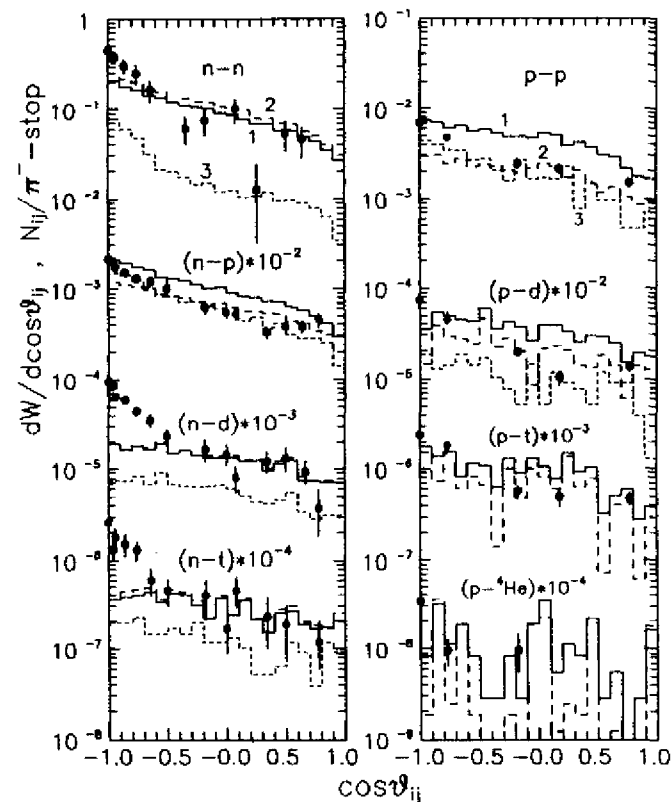


Fig.7. Angular distributions of two coincident fast particles emitted after π^- -absorption in ^{59}Co . The detected particle pairs are indicated in the figure. Points - experimental data [47, 48]. The solid (1) and the dashed (2) histograms show CEM calculations for $R' = 1$ and 6, respectively. The dotted histograms (3) denote for $n-n$ pairs the contribution of the two primary neutrons, and for the rest pairs show the CEM prediction for events when a primary nucleon is detected in coincidence with the second fast particle ($R' = 1$).

From our point of view, these discrepancies are mainly caused by neglecting in the present version of CEM of such mechanisms of composite particle emission, as, pick-up, knocking-out, or final state interactions at the cascade stage of reaction resulting in coalescence of nucleons into a composite particle, rather than by neglecting here the absorption of pions on α and other heavy clusters. As a confirmation of this may be looked our CEM calculations of composite particle emission in proton-nucleus reactions at $E_0 = 29, 62, 90$ and 100 MeV [39, 41]. For these reactions

the CEM satisfactorily describes composite particle emission at large angles, while at small angles the fast composite particle yields are greatly underestimated. For proton-nucleus reactions this testifies just to the mentioned above but neglected on calculating mechanisms of composite particle production.

An indication for a some small fraction of pion absorption on heavier clusters is regarded here nucleus-target ^{58}Co may be found from comparison of $(n-d)$ and $(n-t)$ angular correlations with $(p-d)$ and, respectively, $(p-t)$ ones. So, as is seen from fig.7, CEM predicts the same shape of angular correlations for $(n-d)$ and $(p-d)$, or for $(n-t)$ and $(p-t)$ pair ("works" only the kinematics). While, the experimental $(n-d)$ and $(n-t)$ angular correlations are sharper than $(p-d)$ and $(p-t)$ ones. This may indicate on some part of direct d and t in $(n-d)$ and $(n-t)$ detected pairs from the absorption of pions on ^3He and α -clusters, respectively. Note that the upper limit for the probability of the primary pairs emitted after pion absorption in ^{58}Co and ^{197}Au measured in [48] is of $0.15/\pi^-$ - stop. This fact directly notes on a small fraction of pion absorption on heavy clusters in medium and heavy nuclei-targets.

Table 3

Yields of two coincident particles emitted after π^- -absorption in ^{58}Co [N_{ij}/N_{π^-}] for $E_{n,p,d,t} > 20$ MeV and $E_{^3\text{He},\alpha} > 35$ MeV. The numbers in brackets show the statistical error on the last digits.

| Emitted particles | Exp. [47],[48] | CEM (present work) | | | |
|------------------------------|----------------|--------------------|---------------|-----------|-----------|
| | | $R' = 0$ | $R' = \infty$ | $R' = 1$ | $R' = 6$ |
| $n-n$ | .19(4) | .081(1) | .238(2) | .193(1) | .278(1) |
| $n-p$ | .14(3) | .431(2) | .114(1) | .206(2) | .134(1) |
| $(n-d) \cdot 10^1$ | .4(1) | .236(5) | .272(7) | .259(6) | .270(7) |
| $(n-t) \cdot 10^2$ | .9(3) | .416(20) | .650(35) | .582(30) | .635(34) |
| $(n-^3\text{He}) \cdot 10^3$ | | .611(76) | .458(92) | .502(87) | .467(91) |
| $(n-\alpha) \cdot 10^3$ | | .659(79) | 1.04(14) | .906(129) | .984(132) |
| $(p-p) \cdot 10^2$ | .54(10) | 2.55(3) | .242(20) | .905(16) | .388(16) |
| $(p-d) \cdot 10^2$ | .46(9) | 1.57(4) | .335(25) | .692(29) | .413(26) |
| $(p-t) \cdot 10^2$ | .17(3) | .363(19) | .123(15) | .192(16) | .138(15) |
| $(p-^3\text{He}) \cdot 10^4$ | .25(10) | 1.43(37) | <.183 | .414(107) | .091(24) |
| $(p-\alpha) \cdot 10^3$ | .12(4) | .449(66) | .128(48) | .221(53) | .148(50) |
| $(d-d) \cdot 10^3$ | .90(19) | .315(39) | .201(43) | .233(42) | .208(43) |
| $(d-t) \cdot 10^3$ | .47(10) | .193(43) | .165(55) | .172(51) | .166(54) |
| $(d-^3\text{He}) \cdot 10^4$ | .2(1) | .096(96) | <.183 | .028(28) | .006(6) |
| $(d-\alpha) \cdot 10^4$ | .85(30) | .286(165) | .366(259) | .343(232) | .361(253) |
| $(t-t) \cdot 10^4$ | .6(2) | .191(96) | .273(159) | .251(141) | .269(155) |
| $(t-^3\text{He}) \cdot 10^4$ | .05(5) | .286(165) | <.183 | .083(48) | .018(11) |
| $(t-\alpha) \cdot 10^4$ | .15(10) | <.096 | .183(183) | .130(130) | .171(171) |
| $(\alpha-\alpha) \cdot 10^4$ | <.05 | <.048 | <.092 | <.065 | <.081 |

3.5. Analysis of the Experimental Correlation Data for the "Live" Target

The main difference between Gornov *et al.* experiments [18]-[22] and the experiments performed earlier is the use of the "live" target. The particles produced were recorded by telescopes of Si

detectors. As the silicon target the authors used a $\text{Si}(\text{Au})$ semiconductor detector, which was a "live" target. The energy release in the target is the result of the energy loss by the pion and by the recorded particle, and also by the recoil nucleus and other unrecorded particles emitted by the nucleus. A monitor system consisting of two semiconductor detectors [54] permits determination of the pion energy on entry into the target and correspondingly of the depth of pion penetration in the target. Using these data, from the energy release in the target the authors subtracted the contribution of the pion and of the recorded particle. The use of the detector as a target permitted Gornov *et al.* to measure correlation data and the Monte Carlo CEM method permitted us to analyze them [18]-[22].

Figure 8 shows the spectrum of energy released in the target when protons are detected in the energy range 40-70 MeV.

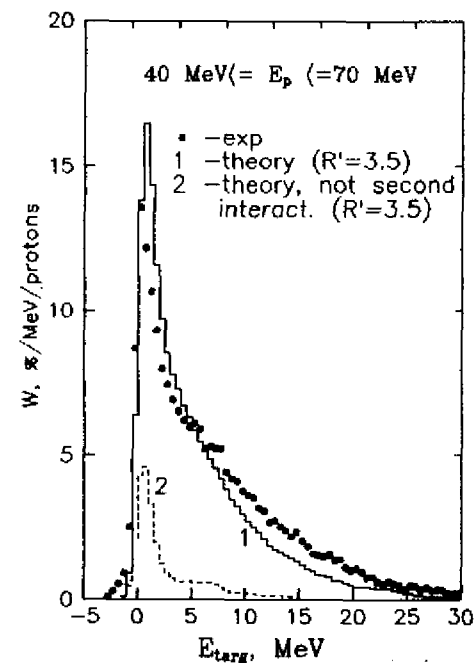


Fig.8. The spectrum of energy released in the "live" target on recording protons in the energy range 40-70 MeV. Points - experimental data [22], solid histogram - CEM calculation, dashed histogram - CEM calculation for events without interactions in the nuclear interior ($R' = 3.5$).

The experimental and theoretical data were normalized to the area per detected particle. It is clear that this correlation characteristic is also reproduced by the CEM calculations. The most characteristic feature of these distributions is the sharp peak at low values of released energy. The theoretical distribution corresponding to events in which primary particles (proton and neutron)

e emitted from the nucleus without interaction is shown separately. This distribution is normalized to the relative probability ($\approx 20\%$) of such events. The fraction contributed by the peak in this distribution is $\approx 65\%$. Calculations have shown [18] that the distributions for events in which at least one of the primary particles has undergone an interaction in the nucleus does not have this structure. Hence it may be concluded that the region of the peak on the experimental distribution corresponds to events that involve mostly the emission of two primary particles.

To enable the authors to extract the primary proton spectra, the experimental distributions obtained with the "live" target were approximated [18, 20, 22] by the sum of two functions, namely, a normal function with an average value in the region of the low energy release, and a polynomial describing the remainder of the spectrum. This procedure was acceptable for sufficiently narrow energy intervals, for which this approximation gives stable results and the theoretical χ^2 . By considering the contribution of the normal distribution as the fraction of events with the emission of two primary particles, the authors are able to reconstruct the spectrum of primary protons from absorption events. Figure 3 shows the resulting spectrum of primary protons together with the CEM spectrum calculated for $R' = 3.5$. As can be seen, the theoretical and experimental distributions are in good agreement up to 90 MeV. At higher energies, the differences between the spectra obtained with the "live" target from different particle-emission mechanisms are practically imperceptible, which naturally restricts the energy range of this method.

The above procedure of extracting the spectrum of primary protons can serve as an independent method of determining R' . For Gornov *et al.* data [18, 20, 22] the value of R' obtained in this way turned out to be 3.5, i.e., equal to the average value found by analyzing inclusive spectra. It is important to note that the determination of R' from the fraction contributed by the primary-particle peak is not very dependent on the absolute experimental uncertainties. This is particularly important for large value of R' , for which the inclusive yield of protons is a slowly-varying function of R (5), whereas the yield of primary protons is inversely proportional to R .

In figure 9 we have shown the spectra of the energy release in the target normalized per recorded particle for reactions with emission of deuterons and tritons. One can see an appreciable disagreement between the shapes of the CEM and experimental distributions. The differences manifest themselves, mainly, in the presence in the experimental spectra of a peak near zero energy release. As was mentioned above this region corresponds to "direct" processes which occur with no excitation of the nucleus and with no subsequent emission of charged particles.

For deuterons the peak appears most distinctly [20] at energies 30-70 MeV, which corresponds to the region of the maximum of the energy distribution of the primary nucleons in the two-nucleon absorption mechanism. Note that in this energy range the shapes of the spectra of the energy release in the "live" target for deuterons (fig.9) and for protons (fig.8) are practically identical. These circumstances are consistent with the assumption that an appreciable fraction of deuterons is produced as the result of two-nucleon absorption and subsequent pickup in the surface layer of the nucleus [28].

The spectra of the energy release in the target for tritons differ from those for protons and neutrons, which possibly is caused by a different mechanism of their formation. For tritons the maximum in the region of small energy releases is not as distinct, but nevertheless the deviations from the CEM calculation are still substantial. In this case it is difficult to draw any conclusion in favor of the pickup mechanism, particularly if we take into account that the maximum in the region of small energy releases is seen most clearly for tritons with energies of about 30 MeV [20], i.e., in the region corresponding to absorption of the pion by an intranuclear quasi-free α particle.

The differences observed in the experimental and computed spectra of the energy release in "live" target on recording deuterons and tritons are rather distinct and permit one on the basis of

the portion of events with small energy release to estimate the contribution of "direct" processes to the formation of composite particles to be at a level 20-40% [18, 21].

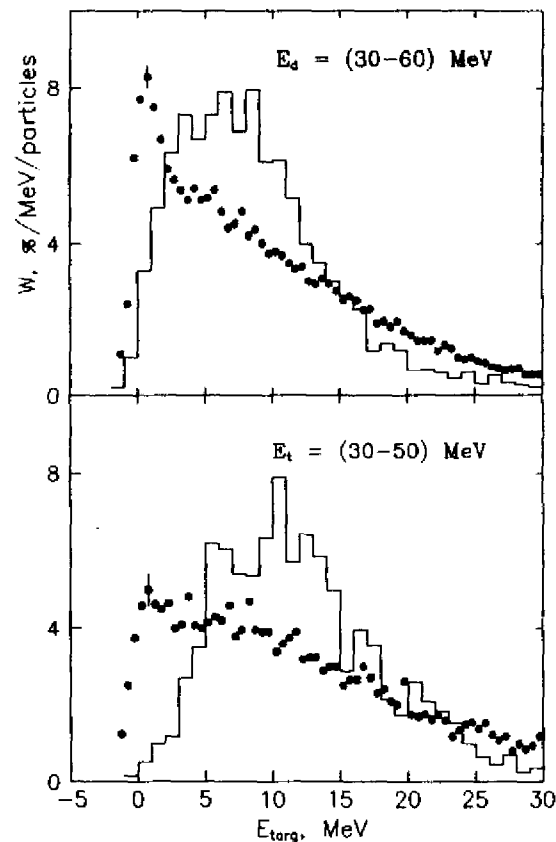


Fig.9. Spectra of the energy release in the "live" target on recording deuterons and tritons in the energy range 30-60 MeV and 30-50 MeV, respectively. The points are the experimental [21], and the histograms are the CEM calculation ($R' = 3.5$).

We should emphasize that this conclusion is independent of the absolute normalization of the experimental data. As is seen from figure 4 and tables 2 and 3, an observation of the additional mechanisms of the composite-particle production is consistent with the difference in the experimental and predicted by the CEM absolute yields of composite particles, particularly if we take into account the accuracies of the measurement and calculation (about 20-30 %).

3.6. Isotope Yield

This is an important characteristic of pion absorption in nuclei, dealt with in many experimental studies (see, for example, review [2]).

The experimental data show that pion absorption is accompanied with strong nuclear spallation. Thus, in case of medium or heavy nucleus the number of emitted nucleons may achieve 15-17, which corresponds to the excitation energy close to the pion mass. Here, multiplicity distribution is wide and ranges from 2 to ~ 16 particles. This distribution can be easily explained by our CEM. Indeed, since the energy of cascade particles ranges widely (fig.1), then the excitation energy distribution of residual nuclei will be wide too. Our calculations [32, 41] show that in the CEM the mean excitation energy of the residual nuclei after the cascade stage of the reaction increases with increasing mass number A of the nucleus-target. Therefore, the heavier is the nucleus-target, the wider the isotope yield, as increases the number of slow particles emitted at the pre-equilibrium and evaporative stages of reaction.

As an example, in figure 10 the experimental yields [55] of the reactions $^{59}\text{Co}(\pi^-, \gamma p x n)$ are compared with calculations performed by cascade-evaporation [4], exciton [55] and our cascade-exciton models. A similar agreement between theory and experimental data was obtained also for other nuclei [26].

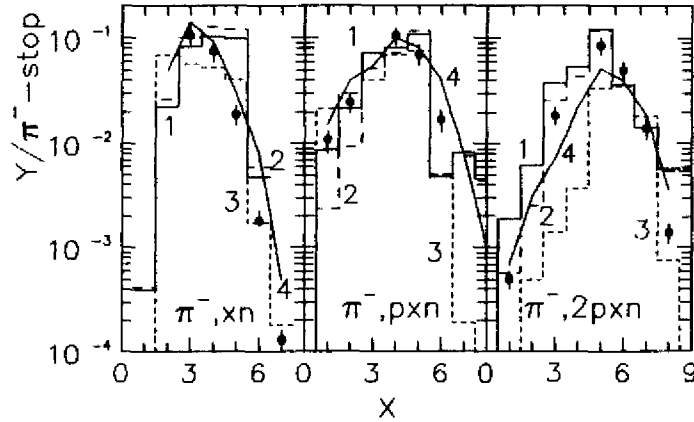


Fig.10. Isotope yield following pion absorption by ^{59}Co nuclei. Experimental data are from [55]. The solid (1) and dashed (2) histograms - CEM calculations for $R=1$ and 6, respectively; point histograms (3) - cascade-evaporation model calculation from [4]; solid curve (4) - exciton model calculation from [55].

One can see, that the models are equally successful in describing the main feature of nuclear disintegration following π^- -absorption. This may be explained by a great contribution of the evaporation stage, which is present in all models and is equally described, to the production of the given final isotope. By the great contribution of the pre-equilibrium and evaporative processes may be explained also the weak dependence of the theoretical isotope yield on the value of R (fig.10).

3.7. Excitation of High Spin States and Angular Momenta of Residual Nuclei

It is found in [56] that following pion absorption in heavy nucleus-target metastable states of residual nuclei whose spin achieves 10-20 \hbar are excited intensively. These experiments excite great interest. It was unclear how such high angular momentum of residual nuclei appear, if the orbital momentum, l_π , of the pion on the mesoatomic orbit from which absorption occurs, is small ($l_\pi \leq 3\hbar$). Therefore, a great number of experiments dealing with this phenomenon have been performed for a short time (see review [2]).

This phenomenon has been explained by Iljinov *et al.* [37]. Later its similar interpretation has been given by other authors (see review [2]). It is shown that most nucleons emitted from the surface layer of the nucleus at the stage of an intranuclear cascade are responsible for the large angular momentum of the residual nucleus. In the case of heavy nuclei-targets, residual nuclei, whose angular momentum may achieve 15-17 \hbar , are produced following intranuclear cascade stage. High angular momenta of residual nuclei such as these are comparable with ones obtained in reactions with heavy ions may be achieved. While in reactions with heavy ions the angular momentum is introduced by an incident particle, then in reactions with pions the additional angular momentum is created due to emission of fast particles from the surface nuclear layer.

It is clear that CEM also contains this mechanism of high angular momentum for the residual nucleus in pionic absorption. Another mechanism for this phenomenon which is present both in the CEM and the cascade-evaporation and the exciton models is a fluctuation one, when a large angular momentum of the residual nucleus may be produced due to random addition of momenta carried away by evaporated particles. Perhaps, some hints as to such a mechanism may be found in [57] where it is observed that emission of 13 neutrons following pion absorption in ^{181}Ta nucleus excite the states with the spin 16 \hbar (with the probability $\sim 10^{-3}$ per 1 pion).

At least, both the CEM and the exciton models contain the third mechanism for the large angular momentum of the residual nucleus - the emission of fast composite particles (less important - nucleons) at the pre-equilibrium stage of the reaction.

Let us estimate in the CEM the role of pre-equilibrium and evaporative particle emissions as a source of high angular momentum for the residual nucleus. The angular momentum of residual nucleus M is determined in the CEM by the expression

$$M = s + l_\pi - \left(\sum_i m_i^{CAS} + \sum_j m_j^{PREQ} + \sum_k m_k^{EQ} \right),$$

where s is the spin of the target nucleus, l_π is the orbital momentum of the pion in the mesoatomic state from which the pion was absorbed, m_i^{CAS} , m_j^{PREQ} and m_k^{EQ} are the angular momentum taken away by the i th cascade, j th pre-equilibrium and k th equilibrium (compound) particles, respectively. The model of intranuclear cascades considers angular momenta of high-energy nucleons m_i^{CAS} as classical vectors [37]. Since $|\sum_i m_i^{CAS}| \gg 1$ [37], let us, following [27], consider on calculating M as classical also the vectors s , l_π , m_j^{PREQ} and m_k^{EQ} .

Following [27] we will estimate the angular momenta of pre-equilibrium and evaporated particles by the sharp cut-off approximation. Then the distribution of m_j in the interval $[0, m_j^{max}]$ satisfies the expression $W(m_j)dm_j \sim m_j dm_j$, where

$$m_j^{max} = \frac{R_j}{\hbar} \sqrt{2\mu_j(E_j - V_j)}.$$

Here R_j is the radius of the interaction of j th emitted particle with the residual nucleus, E_j , μ_j and V_j are the energy in the centre-of-mass system, Coulomb barrier and reduced mass of the particle, respectively. Distribution over the quantity l_π was taken from the calculations of the atomic cascade [27] (see table 4).

In figure 11 the CEM prediction for the distributions of residual nuclei over the absolute value of the angular momentum is given. It is clear that the main mechanism of nucleus "twisting" is the emission of fast nucleons from the nucleus surface layer at the cascade stage of reaction. As in the cascade-evaporation model [27, 37] a heavy nucleus following π^- -absorption may obtain after the cascade stage of reaction an angular momentum of $18\hbar$ (with a probability of $\sim 10^{-3}$).

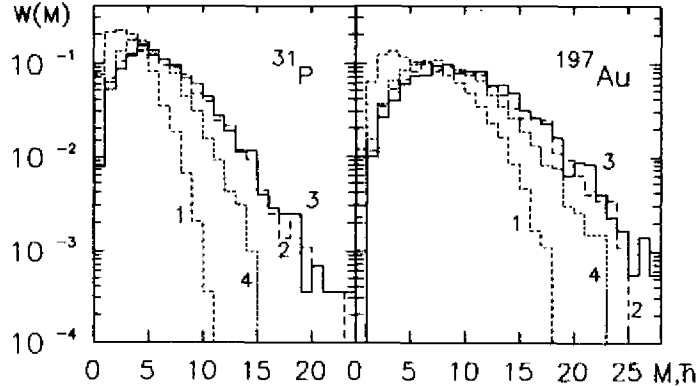


Fig.11. Distribution of the residual nuclei formed after pion absorption in ^{31}P and ^{197}Au over the angular momentum $|M|$. Histograms 1, 2 and 3 show the contribution of cascade, cascade and pre-equilibrium and of all three (cascade, pre-equilibrium and evaporative) CEM components, respectively ($R' = 1$). Histograms 4 denote cascade-evaporation model [27] calculation.

The pre-equilibrium particle emission may increase angular momentum of residual nucleus up to 23-25 \hbar (with a probability of $\sim 10^{-3} - 10^{-4}$). It is clear that pre-equilibrium mechanism of nucleus "twisting" is more important for light nuclei-targets. At the evaporation stage of reaction the angular momentum of residual nucleus may increase by 1 \hbar for light nuclei-targets and, by $\sim 3 \hbar$ for heavy ones (with a probability of $\sim 10^{-3} - 10^{-4}$).

Table 4

A relative portion (in %) of the pion absorption from each l -state of the mesoatom [27]

| Nucleus | l | | | | |
|-------------------|------|-------|-------|-------|------|
| | 0 | 1 | 2 | 3 | 4 |
| ^{31}P | 3.32 | 87.93 | 8.747 | | |
| ^{40}Ca | 1.79 | 69.98 | 28.23 | | |
| ^{59}Co | | 33.89 | 64.69 | 0.36 | |
| ^{75}As | | 16.90 | 80.55 | 1.67 | |
| ^{181}Ta | | 1.73 | 18.61 | 74.98 | 4.01 |
| ^{197}Au | | 1.67 | 12.54 | 77.13 | 7.96 |
| ^{209}Bi | | 1.63 | 9.70 | 75.95 | 12.0 |

3.8. Momentum of Residual Nucleus

Another important characteristic of residual nucleus is its linear momentum P . Within the light nuclei region the absorption products are emitted mainly without interaction with intranuclear nucleons, therefore measurements of the nucleus momentum make it possible to determine the momentum of multinucleon association absorbing a pion. Great contribution of secondary processes accompanying pion absorption in complex nuclei makes the situation more intricate. The momentum of the nucleus-target will depend on different reaction characteristics as, for example, on the number of nucleons emitted ΔA .

For the simplest reaction ($\pi^-, 2n$) the nucleus momentum may be extracted from the analysis of the kinematically complete experiment involving measurement of the energies of two neutrons. Measurement of nuclear momentum in terms of the Doppler effect may be used in general for a wider set of residual nuclei (see review [2]).

In the CEM the momentum of residual nucleus P is determined by the momenta p_i , p_j and p_k of the particles emitted at the cascade, pre-equilibrium and evaporative stages of reaction, respectively

$$P = -(\sum_i p_i^{CAS} + \sum_j p_j^{PREQ} + \sum_k p_k^{EQ}).$$

As an example, in fig. 12 are shown the $|P|$ distributions of residual nuclei formed after pion absorption in ^{40}Ca and ^{209}Bi .

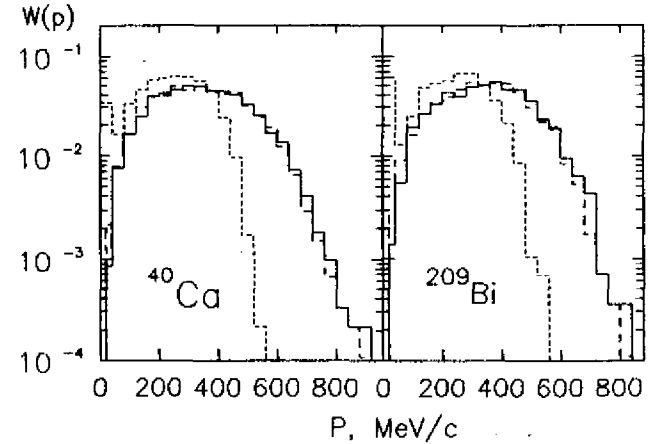


Fig.12. Distribution of the residual nuclei formed after pion absorption in ^{40}Ca and ^{209}Bi over the linear momentum $|P|$. Dotted, dashed and solid histograms denote the contribution of cascade, cascade and pre-equilibrium and of all three (cascade, pre-equilibrium and evaporative) CEM components, respectively ($R' = 1$).

One can see, in contrast to the angular momenta, distributions of the linear momenta of residual nuclei slightly depend on the nucleus-target. The mean momentum of the residual nucleus calculated in the CEM does not practically depend on the mass number of the nucleus-target and is equal to $\bar{P} \approx 350 \text{ MeV/c}$. The emission of particles at the pre-equilibrium stage of reaction

performs a considerable role in the production of high momentum residual nuclei.

The importance of pre-equilibrium emission may be also observed in fig.13, where the calculated dependence of the mean nucleons momentum \bar{P} vs the number, ΔA , of nucleons, removed from the target following pion absorption in it, is compared with experiment. One can see, the results of calculation in the case of no pre-equilibrium emission and evaporation lie below the experimental \bar{P} values at high ΔA . The consideration of the momenta of pre-equilibrium and evaporated particles improves the agreement with the experiment.

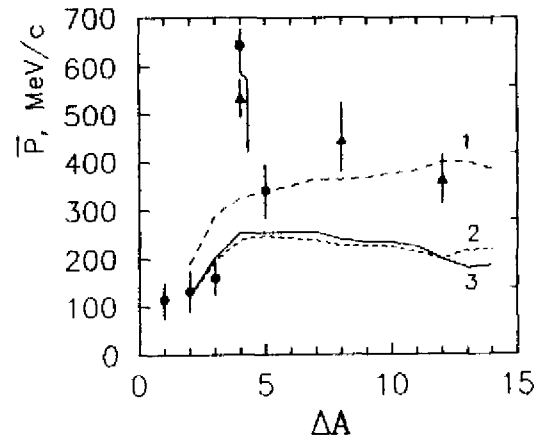


Fig.13. Dependence of the average momentum of the residual nucleus $|\bar{P}|$ on the number of nucleons ΔA emitted from the target nucleus. Experimental data for ^{31}P (circles) and ^{40}Ca (triangles) are from [58, 59]. Solid (3) and dotted (2) curves - cascade calculations from [4] for ^{40}Ca and ^{31}P , respectively ($R' = 1$). Dashed (1) curve - CEM calculation for ^{40}Ca ($R' = 1$).

4. Conclusion

The results represented above show that CEM may be used to describe a large variety of characteristics of stopped negative pion absorption by intermediate and heavy nuclei and to estimate the contribution of different pion absorption mechanisms and the role of different particle production mechanisms in these reactions.

The analysis of experimental data performed in this work shows that in pion absorption the two-nucleon mechanism is the main one. The probability for single nucleon absorption does not exceed $10^{-3} - 10^{-4}$. The problem of the contribution of more complicated absorption mechanisms, for example, the α -particle one, is still open. The presence of these mechanisms may be indicated by the discrepancy obtained between theory and experiment for the spectra, angular correlations and yields of composite particles. We have obtained [18, 21] a direct indication on the α -particle absorption mechanism in ^{28}Si from the analysis of spectra of energy release in the target for reactions with emission of tritons.

The CEM predicts a noticeable yield of composite particles due to the pre-equilibrium emission mechanism. At the same time, our investigations show that pre-equilibrium emission and evaporation are not the only mechanism of composite particles production. From our point of view, various mechanisms "work" in production of composite particles, and the different behavior of A dependence of their yields, probably, manifests various mechanisms of their formation. From the differences observed in the experimental and CEM spectra of energy release in the "live" target on recording deuterons and tritons, on the basis of the portion of events with small energy release, we have estimated the contribution of "direct" processes to the formation of composite particles to be at a level of $\sim 20 - 40\%$ for ^{28}Si target [18, 21].

We have shown that emission of particles at the pre-equilibrium stage of reaction performs a considerable role in the production of high angular and linear momenta of residual nuclei.

The CEM analysis [26] of the old experimental proton spectra measured for various target by different groups [11]-[16], [47] has shown that either the ratio of the widths of elementary processes on np and pp pairs (denoted R') is sensitive enough to nuclear structure of targets, or there are significant contradictions between the absolute normalization of proton spectra measured by different authors. The recent Gornov *et al.* experimental data [22] on the emission of protons by Be , C , Si , Cu and Ge nuclei are consistent with the assumption that R' remains constant in a wide range of nucleon masses (from carbon to copper). The result $R' = 3.5 \pm 1.5$ obtained here from analysis of different characteristics (inclusive proton spectra, ratio of high-energy proton and neutron yields and correlation measurements using the "live" target) is very close to the value obtained [52] for ^3He , i.e., the lightest nucleus for which absorption by both np and pp pairs is possible. To clarify finally this question, further measurement on the other targets, especially different isotopes of the same elements, would be useful. We suggest [22] to use the dependence of the proton yield on the probability of absorption on pp pairs to systematize experimental results.

Acknowledgments

Many of results presented here have been obtained in common work with Professors V.D. Toneev and A.I. Ijginov, and Doctors K.K. Gudima, S.E. Chigrinov, B.A. Chernyshev, E.A. Cherepanov and V.N. Nazarov and my thanks go to each of them. Recently I have happily collaborated with a big group of experimenters from Moscow Engineering-Physics Institute - Leningrad Institute of Nuclear Physics - JINR Collaboration headed by Doctor M.G. Gornov. I am grateful to all them for useful collaboration and to Doctor M.G. Gornov for many fruitful discussions. I wish to thank Professor M. Blann for helpful discussions.

I would like to thank Professor Abdus Salam, the International Atomic Agency and UNESCO for support and hospitality at the International Centre for Theoretical Physics, Trieste.

References

- [1] J. Hüfner, Phys.Rep. 21 (1975) 1.
- [2] V.S. Butsev, A.S. Iljinov and S.E. Chigrinov, Fiz. Elem. Chastits At. Yadra 11 (1980) 900 [Sov. J. Part. Nucl. 11 (1980) 358].
- [3] B. Bassallesck et al., Nucl. Phys. A319 (1979) 397.
- [4] A.S. Iljinov, E.A. Cherepanov, S.E. Chigrinov and S.G. Masnnik, Preprint INR P-0156, Moscow, 1980.
- [5] V.S. Butsev and D. Chultem, Phys. Lett. B67 (1977) 33.
- [6] V.M. Abasov et al., JINR preprint, D6-11574, Dubna, 1978.
- [7] A.B. Migdal, O.A. Markin and I.N. Mishustin, Zh. Eksp. Teor. Fiz. 70 (1976) 1952 [Sov. Phys. JETP 43 (1976) 830].
- [8] M.A. Troitskii, M.V. Koldaev and N.I. Chekunaev, JETP Letters 25 (1977) 123; Zh. Eksp. Teor. Fiz. 73 (1977) 1258.
- [9] P.J. Castelberry et al., Phys. Lett. B34 (1971) 57.
- [10] Yu.G. Budyashov et al., Zh. Eksp. Teor. Fiz. 62 (1972) 21 [Sov. Phys. JETP 35 (1972) 13].
- [11] F.W. Schleputz et al., Phys. Rev. C19 (1979) 135.
- [12] G. Mechttersheimer et al., Nucl. Phys. A324 (1979) 379.
- [13] H. Randroll et al., Nucl. Phys. A381 (1982) 317
- [14] H.S. Pruys et al., Nucl. Phys. A252 (1981) 388.
- [15] H.P. Isaak et al., Nucl. Phys. A392 (1983) 385.
- [16] C. Cernigoi et al., Nucl. Phys. A411 (1983) 382.
- [17] C. Cernigoi et al., Nucl. Phys. A456 (1986) 599.
- [18] M.G. Gornov et al., Preprint No. 1116, Leningrad Institute of Nuclear Physics, Leningrad, 1985.
- [19] M.G. Gornov et al., Preprint No. 1185, Leningrad Institute of Nuclear Physics, Leningrad, 1986.
- [20] M.G. Gornov et al., in: "Elementary Particles and Atomic Nuclei", Moscow Engineering-Physics Institute, Moscow, "Energoatomizdat", 1986, p.60.
- [21] M.G. Gornov et al., Yad. Fiz. 47 (1988) 1193 [Sov. J. Nucl. Phys. 47 (1988) 760].
- [22] M.G. Gornov et al., Yad. Fiz. 47 (1988) 959 [Sov. J. Nucl. Phys. 47 (1988) 612].
- [23] H.C. Chiang and J. Hüfner, Nucl. Phys. A352 (1981) 442.
- [24] H. Machner, Nucl. Phys. A395 (1983) 457.
- [25] M. Biann, Phys. Rev. C28 (1983) 1648; C28 (1983) 2286.
- [26] S.G. Mashnik, in: Proc. of the 20th Winter School of the Leningrad Institute of Nuclear Physics, Leningrad, 3 (1985) 236.
- [27] A.S. Iljinov, M. Leon, R. Seki and S.E. Chigrinov, Preprint INR P-0188, Moscow, 1981.
- [28] F. Hachenberg, H.C. Chiang and J. Hüfner, Phys. Lett. B97 (1980) 183.
- [29] F. Hachenberg, Phys. Lett. B113 (1982) 451.
- [30] V.M. Datar and B.K. Jain, Phys. Rev. C26 (1982) 616.
- [31] A.S. Iljinov, V.N. Nazaruk, S.G. Mashnik and S.E. Chigrinov, Short Communications in Physics, FIAN 1 (1979) 14 [Soviet Physics-Lebedev Institute Reports 1 (1979)].
- [32] K.K. Gudima, S.G. Mashnik and V.D. Toneev, in: Proc. 8th Int. Conf. High Energy Phys. and Nucl. Str., Vancouver, Canada, 1979. Abstracts, 4A20, 1979, p.79; S.G. Mashnik, in: "Microscopic Calculations of Nuclear Structure and Nuclear Reactions", Kishinev, "Shtiintsa", 1980, p.76; in: "Particles and Nuclei Collisions with Nuclei at Intermediate and High Energies", Kishinev, "Shtiintsa", 1984, p.33.
- [33] V.M. Datar and B.K. Jain, in: Proc. Int. Conf. Nucl. Phys., Berkeley, California, 1980. Abstracts, LBL-1111, 1980, p.94.
- [34] V.M. Kolybasov and V.A. Tsepov, Yad. Fiz. 14 (1971) 744 [Sov. J. Nucl. Phys. 14 (1971) 418].
- [35] D.F. Jackson and D.J. Berner, Prog. Part. Nucl. Phys. 5 (1981) 143.
- [36] M. Dörr et al., Nucl. Phys. A445 (1985) 557.
- [37] A.S. Iljinov, V.I. Nazaruk and S.E. Chigrinov, Nucl. Phys. A268 (1976) 513.
- [38] A. Chatterjee and S.K. Gupta, Z. Phys. A307 (1983) 269.
- [39] K.K. Gudima, S.G. Mashnik and V.D. Toneev, Nucl. Phys. A401 (1983) 329; JINR communications P2-80-774; P2-80-777, Dubna, 1980.
- [40] R. Engfer et al., At. Data Nucl. Data Tables 14 (1974) 509.
- [41] S.G. Mashnik, Thesis, Lab. Theor. Phys., JINR, Dubna, 1981.
- [42] R. Madey et al., Phys. Rev. C25 (1982) 3050.
- [43] R. Hartman et al., SIN preprint PR-78-005, Villigen, 1978; Nucl. Phys. A300 (1978) 345.
- [44] H.P. Isaak et al., Nucl. Phys. A392 (1983) 368; H.P. Isaak, Ph. D. thesis, Universität Zürich, 1981.
- [45] H.I. Amols et al., SIN Newsletter 11 (1979) 67; Nucl. Phys. A381 (1982) 317.

- [46] N.S. Mukhopadhyay, J. Haderman and K. Junker, SIN preprint PR-77-017, 1977; Nucl. Phys. A319 (1979) 448.
- [47] U. Sennhauser et al., Nucl. Phys. A386 (1982) 429; A386 (1982) 477; U. Sennhauser, Thesis, ETH-Zürich, 1981.
- [48] P. Heusi et al., Nucl. Phys. A407 (1983) 429; H.P. Isaak et al., SIN preprint PR-82-15, Villigen, 1982; P. Heusi, Thesis, Universität Zürich, 1983.
- [49] F.E. Bertrand and R.W. Peelle, Phys. Rev. C8 (1973) 1045.
- [50] Z. Lewandowski et al., Phys. Lett. B80 (1979) 350.
- [51] J.R. Wu, C.C. Chang and H.D. Holmgren, Phys. Rev. C19 (1979) 698.
- [52] B. Blankleider et al., Nucl. Phys. A463 (1987) 77.
- [53] C.J. Orth et al., Phys. Rev. C26 (1982) 1561.
- [54] M.G. Gornov et al., Nucl. Instr. Meth. 225 (1984) 42.
- [55] H.S. Pruys et al., Nucl. Phys. A316 (1979) 365.
- [56] V.S. Butzev et al., JETF Letters 24 (1976) 117.
- [57] V.S. Beetz et al., Z. Phys. A286 (1978) 215.
- [58] H.D. Engelhard et al., Nucl. Phys. A258 (1976) 480.
- [59] C.E. Stonach et al., Nucl. Phys. A308 (1978) 290.

